THE AMERICAN MINERALOGIST

JOURNAL OF THE MINERALOGICAL SOCIETY OF AMERICA

Vol. 32 MAY–JUNE, 1947 Nos. 5 and 6

APPLICATIONS OF THE NIGGLI-BECKE PROJECTION FOR ROCK ANALYSES

CHARLES S. BACON. JR.

CONTENTS

Illustrations

Figures

Tables

Abstract

Chemical and modal analyses of igneous, sedimentary, and metamorphic rocks are represented on ordinary graph paper as points in the Niggli-Becke quaternary chemical system of rock classification. The components of the system are al (alumina), fm (iron and magnesium oxides), c (lime), and alk (alkalies). Silica values (si) are plotted as ordinates against the quaternary system. Rules for calculating the points from chemical and modal rock analyses are given.

Graphically outstanding among the petrographic relationships are the different distribution fields of the igneous and sedimentary rocks, the four igneous areas in the si diagram (quartz-bearing rocks, quartz-free feldspathic rocks, feldspathoid bearing rocks, and ultra-femic and theralitic rocks), and the chemical transfers involved in metamorphic and weathering processes.

Introduction

Petrologic studies frequently involve the comparison, differentiation and relation of various rock types, either as regards chemical composition or mineral constituents. This may be done with diagrams or tables. Diagrams are preferable because they are more condensed, more readily comprehended and remembered than a series of numbers.

The tetrahedral system of Niggli (1923) as developed by Becke (1925) is the most comprehensive of all petro-chemical diagrams in that it enables a ready comparison of four major chemical units of rock analyses within a tetrahedrom, and by auxiliary diagrams gives the relation of silica and other constituents to the initial four. The system illustrates graphically the chemical variation of the igneous rocks, and of the sedimentary and metamorphic rocks as well. It is a chemical system but lends itself to the plotting of modal analyses, and thus permits chemico-modal comparisons. Genetic, metamorphic and weathering processes involving chemical change are demonstrated effectively.

The writer is grateful to Dr. A. O. Woodford of Pomona College for valuable suggestions and criticisms in the preparation of the manuscript and diagrams.

History

Graphical representation of rock analyses has been tried by numerous investigators (Iddings (1903), Adams (1914), Grout (1918, 1922, 1925), Von Wolff (1922), Hodge (1924), and Peacock (1931)), and several methods are still in use. The chief difficulty encountered has been the adequate representation of the 8 to 10 main oxides contained in most igneous and metamorphic rocks.

Iddings (1892) used a line diagram to express the relations between silica percentages, plotted as abscissas, and the other chemical constituents of rock analyses, plotted as ordinates. Niggli (1923) used diagrams of the same type to express relationships of silica to alumina, to alkalies, to lime, and to his fm value. At the present time, binary or two-component variation diagrams of this type are in common use.

Compositions of mixtures in a ternary or three-component system can be expressed graphically by a series of points in an equilateral triangle the corners of which represent the pure components. This type of diagram, introduced by Gibbs (1876), has come into general use in physical chemistry for illustrating the relations of ternary systems. In petrology this method was used quantitatively by Lang (1892) to express the CaO, Na_2O and K_2O ratios of the igneous rocks, and by Broegger (1895) to illustrate the relationship of monzonite to nepheline syenite, potash feldspar syenite and lime-rich diorite. Becke (1897) plotted K, Na and Ca in

a quantitative diagram illustrating the systematic chemical variation of the igneous rocks. This was followed by Osann's (1900) ACF system, subsequently improved by Becke (1912) by the addition of secondary triangles (SiUL) to express additional relationships.

In physical chemistry the relations of quaternary or four-component systems have been graphed frequently in top- and side-views of a tetrahedron, the four equidistant corners of which represent the pure components while mixtures of 2, 3 or 4 components are represented by points on the edges, faces and interior of the tetrahedron, respectively. Boeke and Eitel (1923) used this system to compare the chemistry of hornblende and augite. Niggli (1923) introduced the tetrahedron for classifying and comparing the chemical analyses of igneous, sedimentary, and metamorphic rocks (Fig. 1), the four corners representing essentially alumina (al), iron oxides and magnesia (fm), lime (c) and alkalies (alk). Niggli plotted al, fm, c and alk by dividing the tetrahedron into 10 slices each of which is a triangle having the corners al, alk and a definite c/fm ratio. Section I has a c/fm ratio of 5/95; section II of 15/85; section III of 25/75; etc. These triangles were plotted back to back along the al-alk edge, arranged so that sections I and X, II and IX, etc., went together. Five double triangles were required to represent the tetrahedron graphically, each analysis being represented by a point in one of the triangles. Points in the tetrahedron which do not fall in one of the section planes obviously cannot be placed accurately in the diagrams.

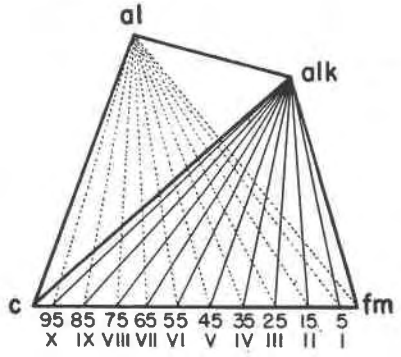

FIG. 1. Niggli tetrahedron showing the original 10 sections.

Becke (1925) rendered the system practicable by setting up the tetrahedron on one edge and viewing it from the top and one side.* In each of these two views the tetrahedron appears as a square cut by two diag-

* This is the crystallographic setup of a tetrahedron. The top and side views are therefore the cubic views 001 and 010, respectively.

onals. The side view is rotated 90° around one edge and placed in contact with the top view (Fig. 2). The analysis points were located in the tetrahedron by 3 coordinates, ξ and η in the top view, and ξ and ζ in the side view. ζ represents the height of the point in the tetrahedron. Becke plotted silica (si) as ordinates against the right side of the top view. He also developed the 6 triangular views of the tetrahedron obtained by sighting along its 6 edges, but made little use of them.*

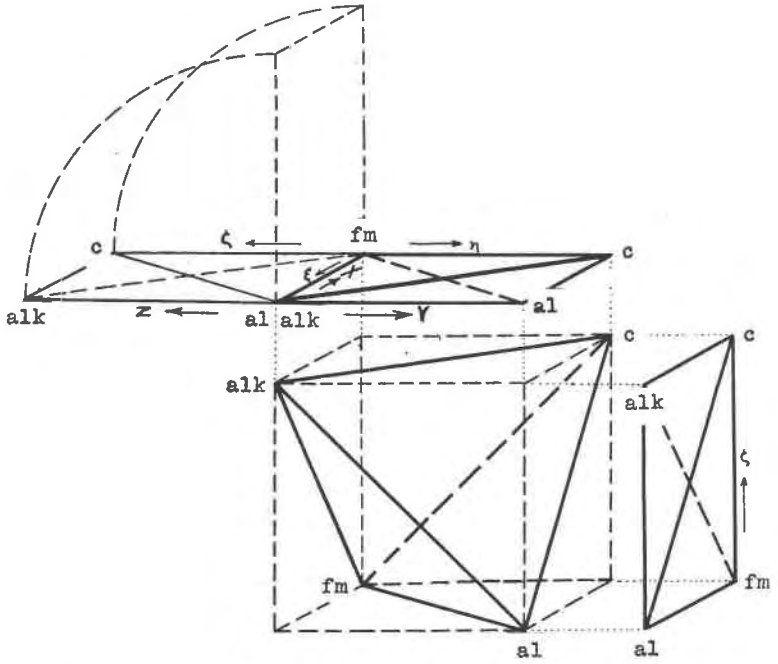

FIG. 2. Derivation of Becke's top and side view method of plotting rock analysis points in the Niggli tetrahedron. The right side view, which gives the elevations of analysis points above the base, is rotated into the horizontal plane and placed to the left of the top view. The newly introduced X, Y and Z coordinates are given in addition to those of Becke.

The photographed model (Fig. 3) of a tetrahedron shows the distribution of igneous rock analysis points. The coordinates X and Y (defined later) are plotted on the base for locating the wire pegs. The lengths of the pegs are equal to Z (defined later). Small wooden balls are slipped on the ends of the pegs to represent the analysis points. The side view is shown in an upright position.

* The triangular views of the tetrahedron are the dodecahedral views 110, $1\bar{1}0$, 011, $0\bar{1}1$, 101 and $\bar{1}01$, or their opposites.

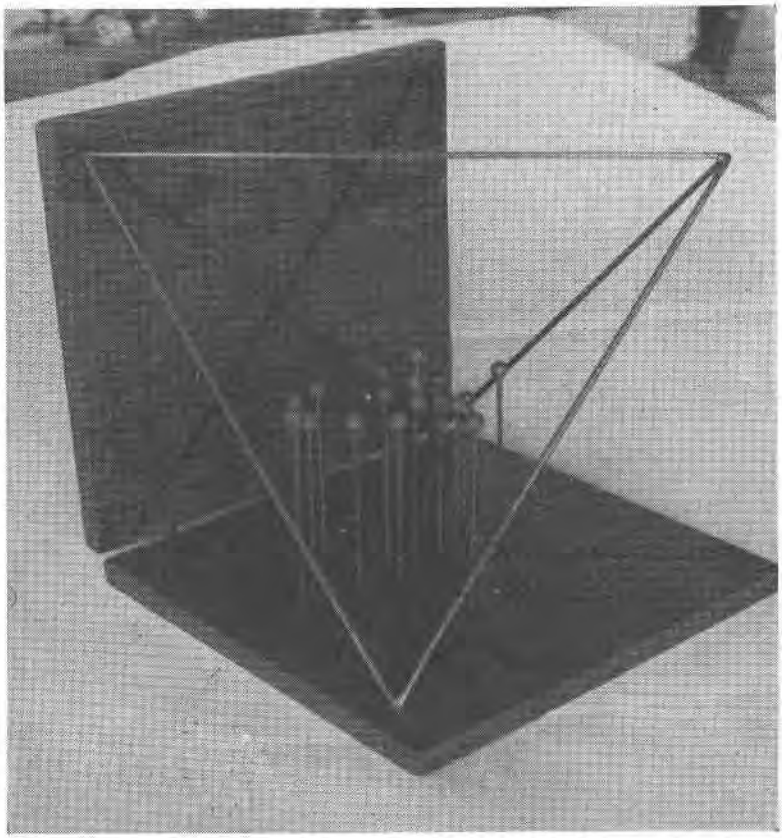

FIG. 3. Model of tetrahedron showing distribution of igneous rock analysis points.

Method of Calculation from the Chemical Analyses

1. Reduce the weight percentage of each oxide of the analysis to the molecular number.

$$\text{Molecular number} = \frac{\text{Weight percentage of the oxide}}{\text{Molecular weight of the oxide*}}.$$

2. If the molecular numbers have been calculated to four decimal places, multiply by 10,000 so as to avoid the use of decimal points in succeeding computations. Enter the figures in a column alongside the weight percentages.

3. Since one molecule of Fe_2O_3 contains twice as much Fe as a molecule of FeO, its molecular number must be multiplied by 2 for sake of proper comparison with the remaining molecular numbers.

4. The molecular numbers are grouped as shown below and then reduced to 100 per cent.

Al_2O_3 (plus any Cr_2O_3 and rare earths)	—al
$Fe_2O_3(\times 2)+FeO+MnO+MgO$ (plus NiO, CuO and other metallic oxides)	—fm
CaO (plus BaO and SrO)	—c
Na_2O+K_2O (plus Li_2O)	—alk
Total	100

5. The coordinate values X, Y and Z are obtained by simple addition and entered in the top and side views of the Becke diagram, hereafter called the *XYZ diagram.*

$$X = c + fm$$
$$Y = c + al$$
$$Z = c + alk.$$

These coordinates replace those of Becke† without change of diagram. From the focus (alk of top view, and al of side view) X increases verti-

* Washington (1917) used whole numbers for the molecular weights of the oxides and suggested that this practice be standardized because of slight changes which are made annually in the tables of atomic weights. The deviations involved are insignificant, and the values used by Washington are given below:

SiO_2	60	MgO	40	H_2O	18	MnO	71
Al_2O_3	102	CaO	56	CO_2	44	BaO	153.5
Fe_2O_3	160	Na_2O	62	TiO_2	80		
FeO	72	K_2O	94	P_2O_5	142		

† X is the reverse direction of ξ and is equal to $100-\xi$. Y corresponds to η and Z corresponds to ζ.

cally, Y increases to the right and Z to the left. The right half of the XYZ diagram will be called the *XY chart*, and the left half will be called the *XZ chart*.

The values al, fm, c and alk can be recalculated from the coordinate values as follows:

$$\text{al} = \frac{100 - X + Y - Z}{2}$$

$$\text{fm} = \frac{X - Y - Z + 100}{2}$$

$$\text{c} = \frac{X + Y + Z - 100}{2}$$

$$\text{alk} = \frac{100 - X - Y + Z}{2}.$$

6. Silica (si) is brought onto an equivalent basis with the Niggli tetrahedral values by the following equation:

$$\text{si} = \frac{\text{Molecular number of } SiO_2}{\text{Sum of the molecular numbers of al, fm, c and alk}}.$$

si is plotted as a variation diagram against X at the right of the XYZ chart using the c-al side as a base. This will be known as the *si chart*, and is the third unit of the diagram which is to be known hereafter as the *XYZ-si diagram*.

7. The values ti (TiO_2), p (P_2O_5), zr (ZrO_2), h (H_2O), co_2, so_3, so_4, cl_2, s, etc. are obtained in the same manner as si. They are not used often.

8. The values k and mg are obtained as follows:

$$\text{k} = \frac{\text{Molecular number of } K_2O}{\text{Molecular numbers of } K_2O + Na_2O \text{ (plus } Li_2O)}$$

$$\text{mg} = \frac{\text{Molecular number of MgO}}{\text{Molecular numbers of } Fe_2O_3\ (\times 2) + FeO + MnO + MgO}.$$

9. k and mg may be plotted as ordinates against X at the left of the XZ chart along the alk-c edge (Fig. 4), and become appendages to the XYZ-si diagram.

10. A salt such as NaCl in the analysis of a sedimentary rock is computed as the oxide of the metallic element. In this case the Na-portion of the molecular number of NaCl is divided by 2 so as to bring it to the same basis for calculation as Na_2O.

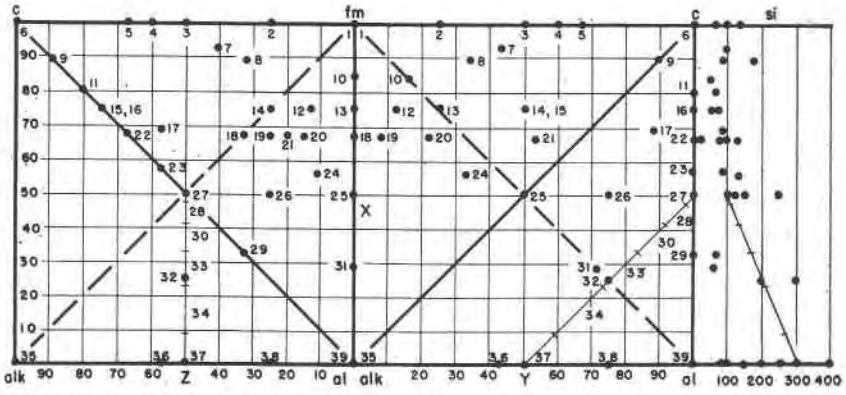

FIG. 4. Mineral distribution in the XYZ-si diagram.

KEY TO MINERALS PLOTTED IN THE XYZ-si DIAGRAM

1 anthophyllite, antigorite, bronzite, brucite, chondrodite, enstatite, epsomite, goethite, hematite, hypersthene, ilmenite, limonite, magnetite, melanterite, olivine, periclase, pyrite, serpentine, siderite, talc, wolframite
2 actinolite, tremolite
3 diallage, diopside, dolomite, hedenbergite
4 andradite
5 akermannite
6 anhydrite, apatite, calcite, collophanite, fluorite, gypsum, perovskite, scheelite, titanite, wollastonite
7 augite
8 hornblende
9 apophyllite
10 chlorite
11 vesuvianite
12 phlogopite
13 almandite, beryl, chamosite, pyrope
14 pargasite
15 polyhalite
16 gehlenite, grossularite
17 allanite, epidote
18 acmite, aegirite, carnallite, riebeckite
19 arfvedsonite
20 biotite
21 xanthopyllite
22 prehnite
23 meionite, zoisite
24 glauconite
25 chromite, cordierite, spinel
26 montmorillonite
27 anorthite, scolecite
28 bytownite
29 margarite
30 labradorite
31 staurolite
32 chabazite, heulandite, phillipsite
33 andesine
34 oligoclase
35 halite, soda niter
36 marialite, sodalite
37 adular, albite, analcite, glaucophane, leucite, microcline, natrolite, nephelite, orthoclase, perthite, sanidine, spodumene
38 alunite, muscovite, paragonite, sericite
39 andalusite, bauxite, beidellite, corundum, diaspore, halloysite, hydrargillite, kaolinite, kyanite, pyrophyllite, sillimanite, topaz

The following example illustrates the method of calculation tabulated in a convenient form. Note the two subtotals ST which added to Al_2O_3 and CaO give the total T.

ROCK ANALYSIS CARD. NIGGLI-BECKE PROJECTION

Name: Granite Analyst: Dr. Karl Willmann
Locality: North side of Echo Lake, Calif. Spec. Grav. 2.663
Reference: *Univ. Calif. Publ.*, Vol. **17**, 1928. Pp. 360–361.

Weight per cent ÷ Mol. Wt. of oxide = Mol. Number (×10,000)					
SiO_2	68.41	60		11,345 ÷ T 3690 = si	308
TiO_2		80		ti	
P_2O_5		142		p	
Al_2O_3	18.05	102		1766 ÷ T 3690 = al	47.9
Fe_2O_3	1.67	160 (×2)	210		
FeO	.71	72	99		
MnO					
MgO	.78	40	194		
			ST	503 ÷ T 3690 = fm	13.6
CaO	2.39	56		426 ÷ T 3690 = c	11.5
Na_2O	3.39	62	547		
K_2O	4.22	94	448		
			ST	995 ÷ T 3690 = alk	27.0
H_2O	.13		T	3690 Total	100.0
H_2O	.16				
Total	99.91				
$K_2O/ST = k$	.45			c + fm = X	25.1
$MgO/ST = mg$	.39			c + al = Y	59.4
				c + alk = Z	38.5

RULES FOR COMPUTING ROCK COORDINATES FROM THE MODES

1. Determine the *tetrahedral factor* TF of each mineral in the rock. From the formula or chemical analysis of the mineral find the weight percentages of the plottable oxides, i.e., those included in the al, fm, c and alk of the tetrahedron. Minerals such as quartz and rutile, lacking in tetrahedral components, are treated later. Divide the weight percentage of each plottable oxide by the molecular weight of the oxide to obtain the molecular number. The sum of the plottable molecular numbers multiplied by the specific gravity of the mineral is the TF of the mineral. Thus, orthoclase contains 64.8% SiO_2, 18.3% Al_2O_3 and 16.9% K_2O by weight. Only the Al_2O_3 and K_2O are plotted in the tetrahedron.* The molec-

* SiO_2 is plotted in the si-chart at the right of the XY chart.

ular ratios corresponding to 18.3% Al_2O_3 and 16.9% K_2O are added (.1794+.1791=.3585) and multiplied by the specific gravity of orthoclase (.3585×2.56=0.92).

The TF of the common rock forming minerals are given (Table 1) so as to eliminate this step from most modal calculations. Many minerals have a constant chemical composition and specific gravity, and consequently a definite TF. Other minerals, including important rock-forming silicates, have variable compositions and specific gravities, and therefore variable TF. The TF figures used in Table 1 are based upon the stated formulas and specific gravities. For best results the TF of such minerals should be based upon individual determinations of composition and specific gravity instead of the averages used in the table. In cases of small volume percentages of such minerals, variations from the average compositions will not displace the rock analysis points appreciably, but where larger percentages are involved accurate values of TF should be obtained.*

2. Multiply the volume percentage of each mineral by the appropriate TF to obtain the molecular number.

3. Reduce the molecular numbers of the minerals with plottable constituents to 100%.

4. Multiply the reduced molecular numbers of the minerals by the factors X, Y, Z and si listed in Table 1.

5. Make summations for X, Y, Z and si, respectively. The position of the rock in the XYZ diagram is given by the totals for X, Y, and Z.

6. Silica (si) is obtained by multiplying the volume percentage of free quartz by the factor 4.42 which is obtained in the same manner as the tetrahedral factors.† The molecular number thus obtained is divided by the sum of the plottable molecular numbers before reduction to 100%. The result is the si for quartz, to which must be added the si of all the other minerals. The si of a mineral such as zircon is obtained in the same manner as for quartz.

7. Other values such as ti, p, zr, h, etc., are obtained in the same manner as si.

The modal calculation of Johannsen's center point granite will serve as an example.

* The hornblende field is scattered between the aluminous pargasite and the ferruginous actinolite, and commonly includes some alkali. Johannsen's (1932) average of a number of analyses of various hornblendes from granites was selected as the center point for hornblende. Johannsen's average of dark mica from 34 granites was chosen for the center point of the biotites. Johannsen's average was used for the center point of augite. The chlorite point corresponds to Dana's (1932) formula of penninite and clinochlore, and falls half way between Becke's (1925) amesite molecule and serpentine.

† $\text{Si factor} = \frac{\text{Weight percentage}}{\text{Molecular weight}} \times \text{Spec. Grav.} = \frac{100}{60} \times 2.656 = 4.42.$

Mineral	Volume %		Tetrahedral Factor	Molecular Number	Plottable Mol. Numbers Reduced to 100%
Quartz	19.9	×	4.42*	88	
Orthoclase	38.1	×	.92	35.0	28.9
Plagioclase ($Ab_{70}An_{30}$)	14.5	×	1.30	18.9	15.6
Biotite	27.5	×	2.44	67.1	55.5
				ST 121.0	ST 100.0

* si factor.

Mineral	Reduced Mol. Nos.	Factors X	Y	Z	si	Rock Values X	Y	Z	si
Quartz	88 / 121								73
Orthoclase	28.9	0	50	50	300	0	14.5	14.5	87
Plagioclase	15.6	23	73	50	240	3.6	11.4	7.8	37
Biotite	55.5	67	22	15	74	37.2	12.2	8.3	41
	ST 100.0				Total	40.8	38.1	30.6	238

Checking the modal calculation

1. Multiply the volume percentages of all the minerals in the rock by their specific gravities and reduce to 100%. These are the weight percentages of the constituents.

2. Multiply the weight percentages by the oxide percentage composition of each mineral and enter the values in tabular form as in the example below. It may be difficult to obtain the correct weight percentages of the complex silicates, and the use of selected or average percentages introduces uncertainties.

3. Add the columns vertically to obtain the chemical composition of the rock.

4. From the chemical composition thus calculated determine X, Y, Z and si according to the method described earlier. These values should

correspond with those obtained from the mode by the regular method.*

Check of the Modal Calculation. (Johannsen's center point granite)

	Volume %	Vol. % ×Spec. Grav.	Wt. %	SiO_2	Al_2O_3	Fe_2O_3	FeO	MgO	CaO	Na_2O	K_2O
Quartz	19.9	52.7	19.4	19.4							
Orthoclase	38.1	97.5	36	23.3	6.6						6.1
Plagioclase ($Ab_{80}An_{20}$)	14.5	38.5	14.2	8.7	3.5				.8	1.2	
Biotite	27.5	82.5	30.4	11.2	5.2	2.3	4.4	2.8	.3	.3	2.5
Total	100.0	271.2	100.0	62.6	15.3	2.3	4.4	2.8	1.1	1.5	8.6
Mol. Nos. ×10,000				10381	1497	288 (×2)	613	694	196	242	913

al	=1497	33.7	X=40.3
fm = 288+613+694	=1595	35.9	Y=38.1
c	= 196	4.4	Z=30.4
alk=242+913	=1155	26.0	si=234

Mineral Distribution in the XYZ-si Diagram†

The mineral distribution in the XYZ-si diagram (Fig. 4) is the key to a thorough understanding of the rock positions and to chemico-modal relationships. Quartz is plotted only as si and has no place in the tetrahedron. The plagioclase feldspar line with its divisions marking the different members of the isomorphous series is the most important feature of Fig. 4. The division points were calculated from analyses given in Winchell (1927), and Tschermak, G. and Becke, F. (1920). The Z of all feldspars is 50. The si ranges from 300 in albite to 100 in anorthite. Located at the same point with the pure albite molecule is orthoclase, nepheline and leucite, but nepheline has an si of only 100 and leucite of 200. The biopyriboles are widely scattered toward the fm corner in both top and side views, with olivine and orthopyroxenes at fm.

Distinctively sedimentary minerals occur at all corners; calcite, gypsum and anhydrite at c, kaolinite and other clay minerals at al, rock salt and soda niter at alk, and the iron ores at fm. Dolomite lies between c and fm.

The minerals of the metamorphic rocks are widely distributed between fm and c, and between al and c.

* The calculated chemical composition of the rock should be compared with a chemical analysis, if available. Such a comparison frequently sheds light on the true compositions of complex silicates which cannot be determined optically. If average compositions of the complex silicates are assumed, the calculated weight percentages may differ notably from the actual analyzed values, and then the true nature of the silicates may be determined and the modal calculation adjusted.

† Printed forms of the XYZ-si diagram and the triangle charts on a single $8\frac{1}{2}\times11$ sheet are available at two dollars per 100 sheets. Sample on request. Address the author.

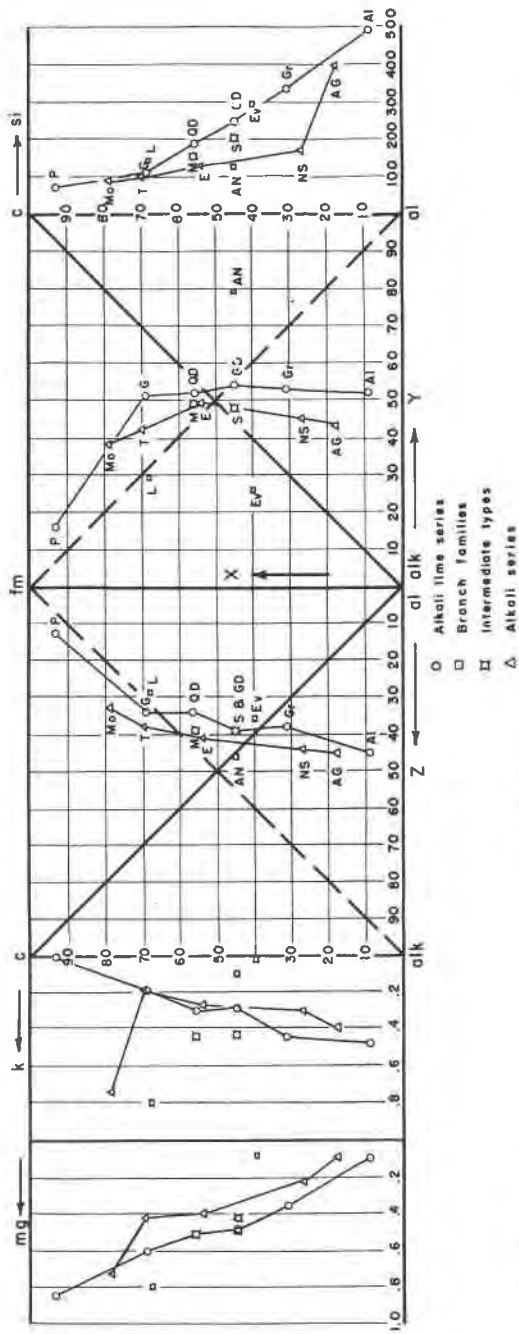

FIG. 5. Average composition of the igneous rocks in the XYZ-si-k-mg diagram.
Rock abbreviations: AG alkali granite, Al alaskite, AN anorthosite, E essexite, Ev evisite, G gabbro, GD granodiorite, Gr granite, L lamprophyre, M monzonite, Mo missourite, NS nepheline syenite, P peridotite, QD quartz diorite, S syenite, T theralite.

Salient Features Illustrated in the XYZ-si Diagram

XY chart: Igneous rocks

The majority of igneous rocks fall into two main groups, the alkali-lime series and the alkali series.* These are distributed in a curved zone from alkali feldspar to the fm corner, the alkali-lime series with higher Y than the alkali series (Becke, 1925) (Fig. 5 and Table 2). The alkali-lime series includes alaskite, granite, granodiorite, quartz diorite, gabbro and peridotite. The alkali series includes alkali granite, nepheline syenite, essexite, theralite and missourite. Two intermediate families, syenite and monzonite, are included, as well as three branch families anorthosite, lamproite and evisite. The Daly (1910) averages are used with the exception of the following family types:

Essexite of Rongstock, Bohemia (preferred by Becke, 1925)
Theralite of Duppau, Bohemia (preferred by Becke, 1925)
Lamproite and evisite (Niggli, 1923)
Alkali granite (average of 13; Osann, 1900)

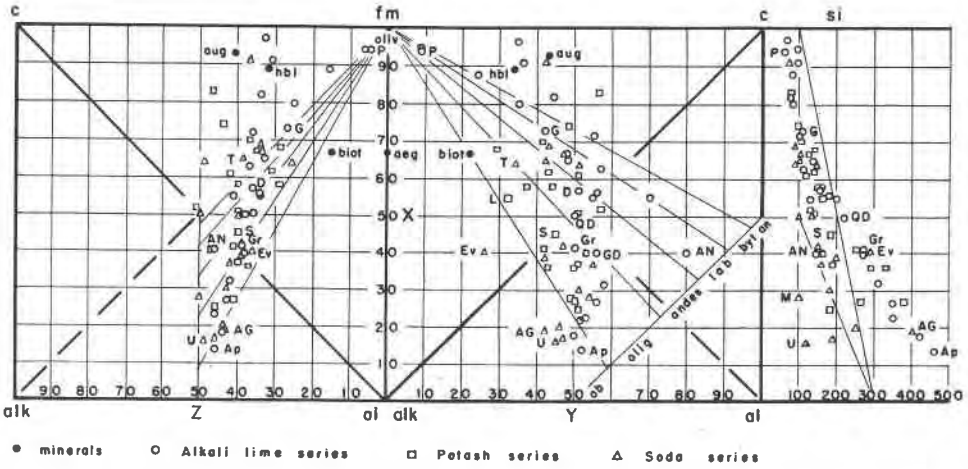

Fig. 6. Niggli's magma families in the XYZ-si diagram.

Minerals: aeg aegirine, aug augite, biot biotite, hbl hornblende, oliv olivine. The plagioclase feldspars are distributed along the line from X 0, Y 50 to X 50, Y 100. The lines converging at fm give the (OrAb)-An ratio of most rocks with X under 70.

Abbreviations of selected families: AG alkali granitic, AN anorthositic, Ap aplite granitic, D normal dioritic, Ev evistic, G normal gabbroid, GD granodioritic, Gr normal granitic, L lamproitic (Wyoming type), M monmouthitic, P peridotitic, QD quartz dioritic, S normal syenitic, T theralitic, U urtitic.

The projection for the anorthosite family lies between those for normal gabbro and for calcic plagioclase. Evisite, the soda-amphibole granite or

* Becke's (1925) Pacific and Atlantic suites respectively.

syenite family, known especially from Evisa, Corsica, is drawn strongly toward the riebeckite point. Lamproite, a family of potash and magnesia rich effusives of lamprophyric character which includes orendite, wyomingite, leucite phonolite and others, is drawn toward fm in consequence of the olivine (and phlogopite) in the rock.

Niggli (1923) grouped the magmas or igneous rock families in three series, the alkali lime series, the potash series, and the soda series (Fig. 6, Table 3). The separation of the two alkali series is not apparent in the XYZ-si diagram but can be demonstrated in a k chart (not shown).

Feldspars largely control the locations of rocks more alkalic than diorite, and the pyriboles predominantly determine the positions of the more femic igneous rocks. A line from fm through the rock analysis point to the feldspar line gives the approximate (OrAb) An (orthoclase-albite anorthite) or the AbAn ratio of the feldspars for rocks more salic than gabbro, the former when both types of feldspars are present, the latter when plagioclase is the only feldspar.* Rocks with soda-pyriboles have unusually low Y which gives the analysis points the appearance of having AbAn ratios in excess of the true values.

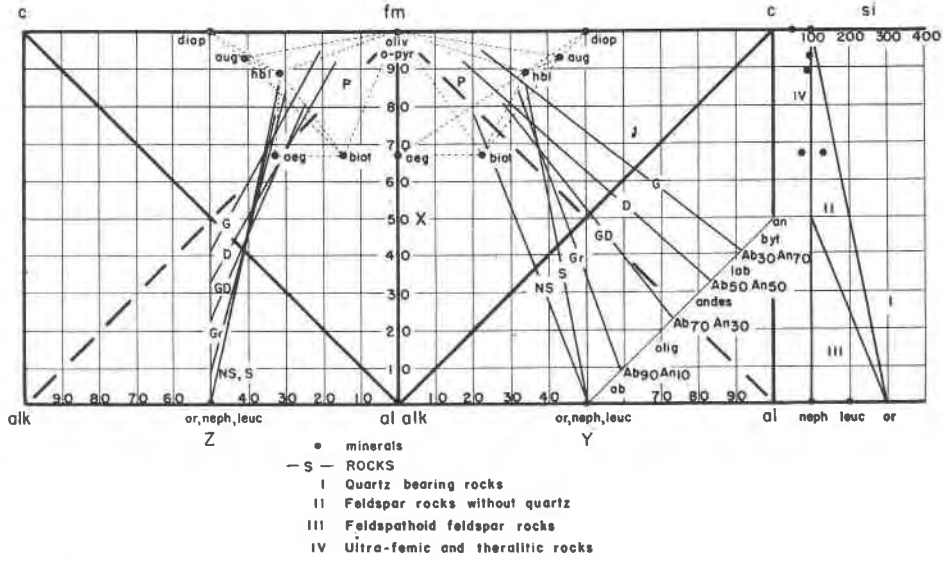

FIG. 7. Modal study of the igneous rocks in the XYZ-si diagram.

Mineral abbreviations: ab albite, aeg aegirite, an anorthite, andes andesine, aug augite, biot biotite, byt bytownite, diop diopside, hbl hornblende, lab labradorite, leuc leucite, neph nepheline, olig oligoclase, oliv olivine, o-pyr orthopyroxene, or orthoclase.

Rock abbreviations: D diorite, G gabbro, GD granodiorite, NS nepheline syenite, P peridotite, S syenite.

* Nepheline and leucite should be included with orthoclase and albite when present.

The families of Johannsen's (1920) quantitative mineralogical classification of the igneous rocks may be plotted like any other modes, but due to the chemical overlap of his families they are not reproduced here, as this would require numerous additional charts.

The distribution of the rocks as controlled by the leading mineral constituents is illustrated in Fig. 7. The average biopyriboles (biotite-pyroxene-amphibole) were calculated for 31 nepheline syenites, 10 syenites, 58 granites, 68 granodiorites, 16 diorites, and 42 gabbros (Johannsen, 1932, 1937, 1938). The XYZ-si of these average biopyriboles and the fields which the points represent are given below:

	X	Y	Z	si	Field
Nepheline syenite	78	20	33	107	aegirite, hornblende, biotite
Syenite	86	34	32	90	hornblende, biotite, augite, diopside
Granite	84	32	30	86	hornblende, biotite, augite
Granodiorite	81	28	25	82	biotite, hornblende
Diorite	92	17	17	92	hornblende, orthopyroxene, clinopyroxene, biotite
Gabbro	95	22	21	84	augite, orthopyroxene, hornblende, olivine

Lines from these points to the proper plagioclases give the linear distributions of the families, the leucocratic members near the feldspar line, the melanocratic members at the other end. Biotite granites are distributed between biotite and albite-oligoclase, whereas hornblende granites have higher Y and lie between hornblende and the same feldspar. The riebeckite granites have lower Y than the biotite granites. Granodiorites, diorites and gabbros lie between the biopyriboles and the plagioclases $Ab_{70}An_{30}$, $Ab_{50}An_{50}$ and $Ab_{30}An_{70}$ respectively. Olivine and orthorhombic pyroxene draw the points for olivine gabbros and norites toward the fm corner. Peridotites and related rocks lie in the triangular area defined by biotite, augite and the fm corner.

The field of the igneous rocks is limited by lines connecting fm, augite, anorthite, albite, aegirite and fm.

XY chart: Sedimentary rocks

The field of the sedimentary rocks in the Niggli tetrahedron has a shape very unlike that of the igneous rocks, due largely to the considerable quantities of lime and alumina in sedimentary rocks (Fig. 8, Table 4).

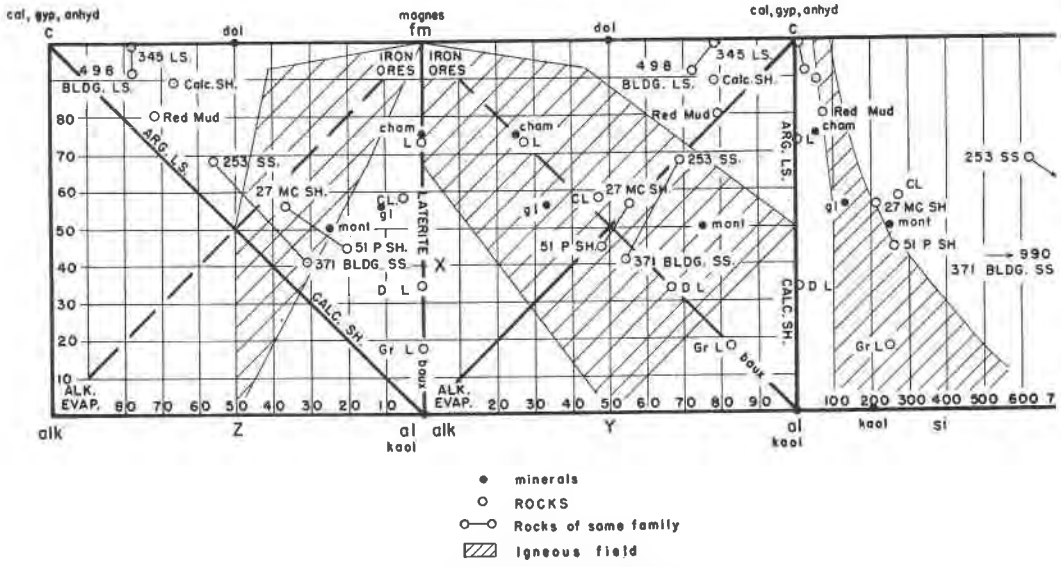

• minerals
○ ROCKS
○—○ Rocks of some family
▨ Igneous field

FIG. 8. Distribution of the sedimentary rocks in the XYZ-si diagram.

Mineral abbreviations: anhyd anhydrite, baux bauxite, cal calcite, cham chamosite, dol dolomite, gl glauconit gyp gypsum, kaol kaolinite, mont montmorillonite.

Rock abbreviations: ALK.EVAP. alkali evaporites, ARG.LS. argillaceous limestones, BLDG.LS. building lim stones, BLDG.SS. building sandstones, CALC.SH. calcareous shales, Calc.SH. calcareous shale, Mt. Diabl Calif., CL clay, D L diorite laterite, Gr L granite laterite, L laterite, LS limestones, MC SH Mesozoic and Cenozo shales, P SH Paleozoic shales, SS sandstones.

Limestones, if pure, lie at the c corner. Most limestones are magnesian, with a little alumina present, and their positions in the diagram are almost, but not quite, on the calcite dolomite line.

Pure kaolin and other clay minerals lie at or near the al corner. Bauxite is usually somewhat ferruginous. Lateritic rocks may contain an fm-al ratio up to more than 2 to 1, occupying the igneous field. Shales lie in the igneous rock field, with an average near that of granodiorite and diorite. Calcareous shales and argillaceous limestones are likely to lie outside of the igneous field, nearer the al-c edge.

Sandstones are distinguished by higher c values than any igneous rocks except anorthosites.

Iron ores lie close to fm. Rock salt and other alkali evaporites lie near alk.

XY chart: Metamorphic rocks

Metamorphic rocks do not occupy an area distinguishable from those of igneous and sedimentary rocks. The mineral combinations in meta-

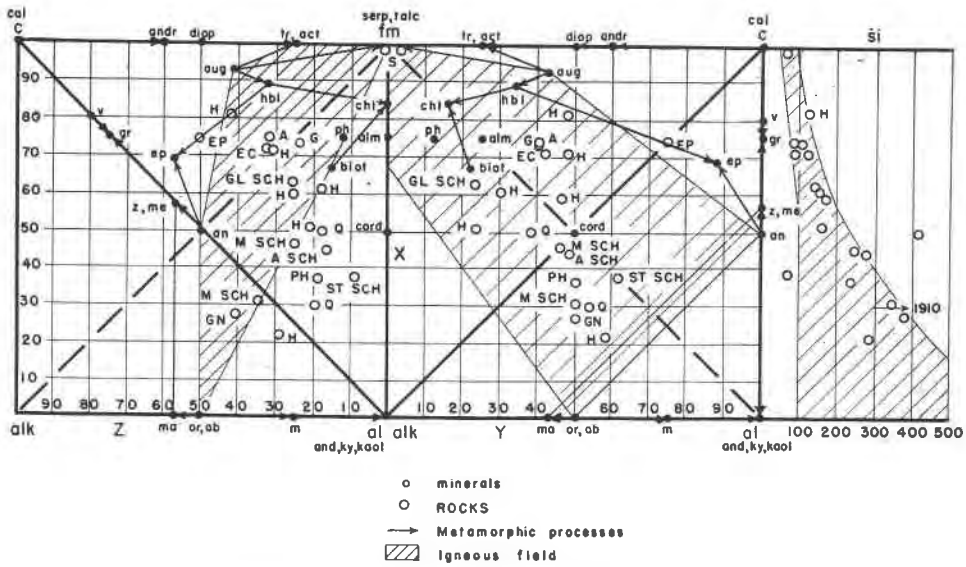

FIG. 9. Metamorphic rocks and processes, and weathering in the XYZ-si diagram.

Mineral abbreviations: ab albite, act actinolite, alm almandite, an anorthite, and andalusite, andr andradite, aug augite, biot biotite, cal calcite, chl chlorite, cord cordierite, diop dicpside, ep epidote, gr grossularite, kaol kaolinite, ky kyanite, m muscovite, ma marialite, me meionite, ph phlogopite, serp serpentine, talc talc, tr tremolite, v vesuvianite, z zoisite.

Rock abbreviations: A amphibolite, EC eclogite, EP epidosite, G greenstone, GL SCH glaucophane schist, GN gneiss, H hornfels, M SCH mica schist, PH phyllite, Q quartzite, ST SCH staurolite schist.

morphic rocks are so varied and numerous so that it is possible to give only the general distribution of a few major rock types (Fig. 9, Table 5).

Slates and some schists differ only slightly from their parent shales and consequently have a similar distribution in the diagram.

Quartzites differ from their parent sandstones in several ways. The calcareous cements of the sandstones may have been replaced by silica. Contact metamorphism may have introduced minerals such as diopside, garnet and wollastonite. Such changes are evident in the diagram by a shift of the analysis points toward the contact minerals.

Contact metamorphosed marble will differ in composition from the parent limestone to the extent that reaction has occurred between the limestone and the magma, magmatic waters or pneumatolytic agents. The analysis points in the diagram will be drawn toward the newly developed minerals.

Gneisses derived from the igneous rocks generally possess the compositions of the parent plutonites, but changes in composition such as

those sometimes attending mylonitization or lit-par-lit injection result in shifts of the analysis points.

Schists differ widely in mineral content and are thus broadly scattered through the tetrahedron. Talc schists, chlorite schists, biotite schists, sericite schists, etc. focus around the dominant constituents but may be widely removed from the corresponding mineral positions if these minerals do not constitute a major portion of the rock.

If a metamorphic rock clearly lies beyond the limits of the igneous rock field, its sedimentary origin is reasonably certain.

XY chart: Metamorphic and weathering processes

A metamorphic change involving the development of new minerals but not attended by chemical transfer cannot be illustrated in the tetrahedron, but changes involving chemical transfers are frequently very prominent. The directions of shift of analysis points accompanying a number of major alteration processes are described below (Fig. 9):

Sericitization involves a loss of Na and generally an increase of K; this is expressed by a shift toward muscovite.

Kaolinization is expressed by a shift toward al due to loss of alk and c.

Alunitization involves loss of all plottable elements except K and Al.

Scapolitization is expressed by a shift from the plagioclase line toward alk and c, especially the latter, in accordance with the usual occurrence in limestone contact zones.

Zoisitization, which may be considered a change from anorthite to zoisite with loss of al, results in an increased X.

Epidotization may be considered a change from anorthite and hornblende towards epidote. The increase in c draws the projection of the rock analysis point toward the epidote point.

Grossularitization is represented as a reaction between plagioclase and limestone, and appears as a double shift from anorthite and c toward the grossularite point. Other types of garnetization may be illustrated in similar manner.

Chloritization may be considered a change from hornblende or biotite toward pennine or clinochlore. It generally involves a loss of alk and of c.

Uralitization is the alteration of pyroxene to amphibole, and its diagrammatic expression depends upon the nature of the particular pyriboles involved. Generally there is a gain in Mg and a loss of Ca which produces a shift toward the fm corner.

Actinolitization involves a change from augite to actinolite. Serpentinization is expressed by shifts from the pyriboles such as diopside, augite

and hornblende toward the fm corner. Olivine and orthorhombic pyroxene, which lie at fm, suffer no change in position when they are altered to serpentine.

Propylitization involves a moderate loss of alk, and a loss of Ca and Mg unless these enter into carbonates or epidote. Commonly propylitization is accompanied by sulfide enrichment (pyrite), and there is relatively little change in X and Y from the original rock.

XZ chart: Igneous rocks

The Z of unaltered igneous rocks is never above 50, and the distribution tapers from fm and the augite position toward the alkali feldspar point in a considerably restricted field (Fig. 5 and 6). The alkali lime series has a distinctly higher Z than the alkali series. Z is greatest for salic rocks with low X, and least for femic rocks with high X. Biotite rocks have lower Z than rocks of the same family containing hornblende or augite.

XZ chart: Sedimentary rocks

Most distinctively sedimentary rocks lie along the al-c edge so that Z increases with X, and the fm content causes the distribution to assume a curved field convex toward fm (Fig. 8). The field of the major sedimentary rocks thus crosses the igneous rock field at a high angle, and sedimentary analyses are rarely similar to igneous ones except at the intersection of the two fields. Bauxite, laterite and the iron ores are low in Z and fall below the igneous field. Many shales have lower Z than igneous rocks, but calcareous shales may lie in the igneous zone. Argillaceous limestones approach the c corner and lie above the igneous rock field.

The calcareous cementing materials of sandstones give to these rocks high c values, and place them above the igneous field. Arkoses and tuffs generally fall in the igneous field.

Rock salt and soda niter lie near the alk corner.

XZ chart: Metamorphic rocks and processes, and weathering

The sedimentary or igneous origin of a metamorphic rock can be recognized provided the projection point of the rock falls outside of the intersection of the two fields of distribution. Rocks above the igneous field (high Z) or below it (low Z) are very likely to have originated as sediments (Fig. 9). Rocks of fairly low X that lie within the igneous field are likely to be of igneous derivation. Sediments injected lit-par-lit or altered to migmatites are not likely to reveal their genesis by the analysis points.

If the origin of a rock is known, the shift in position of the altered rock with respect to its parent illustrates the nature of the chemical changes

that have taken place.

Metamorphic derivatives of the calcareous sediments occupy a field higher in the tetrahedron (greater Z) than the igneous derivatives, whereas aluminous derivatives occupy a lower field (smaller Z) close to the al-fm edge. The former are focused around the points of such minerals as grossularite, andradite, epidote, vesuvianite, gehlenite, etc., while the latter are drawn toward muscovite, kyanite, sillimanite, andalusite, cordierite, chlorite, and others.

The metamorphic processes described for the XY chart can be represented in this chart also.

si chart: Igneous rocks

A line from X 0, si 300 to X 100, si 100, connecting orthoclase and diopside, is the silica saturation or *quartz line* (Figs. 6 and 7). An analysis point with si above this line represents a rock supersaturated with silica and hence probably containing free quartz.

A line from X 0, si 300 to X 50, si 100 is the silica line of the plagioclase feldspars. The triangular field below the quartz line and above the plagioclase line and the si 100 line is that of the quartz-free feldspathic rocks, such as syenites, diorites and gabbros.

Rocks with si values below the plagioclase line have insufficient silica to combine with all of the alumina, lime and alkalies required to form feldspar, and consequently there is a development of feldspathoids. The field between the plagioclase line and the si 100 line is that of the nepheline and leucite syenite rocks.

There are no igneous rocks with si under 100 and X under 50. Those with X over 50 and si under 100 include the peridotites, pyroxenites, dunites, and a few gabbroic rocks with very basic plagioclase.

The si values of the igneous rocks are distributed through a curved zone the upper limit of which extends roughly from X 100, si 50–75 through X 50, si 200 where it crosses the quartz line, to X 10, si 400. When X lies between 0 and 10 the si values may rise much higher, as in the pegmatites. When the feldspar of pegmatites decreases to 0 the si approaches infinity and the rocks grade into quartz veins. The alkali lime rocks generally have distinctly higher si than rocks of the alkali series, and when X is under 50 they generally contain free quartz.

No igneous rocks are known which have high X and high si.

si chart: Sedimentary rocks

Sandstones have exceedingly high si (Fig. 8). The only igneous rocks with equally high si have X under 10, whereas most sandstones have X

well over 50. Shales have si values equal to or slightly higher than igneous rocks of the same X, and the si rises rapidly where the sediments grade into arenaceous and silicified rocks. Limestones, the alkali evaporites, bauxite and laterites have very low si.

si chart: Metamorphic rocks and processes

Silicification, whether hydrothermal or diagenetic, increases the si according to the degree of completion of the process. Silicified rocks are likely to have high si.

Metamorphic rocks differ as greatly in si as their parent rocks (Fig. 9). Metamorphic limestones, chlorite-, talc-, and biotite schists, amphibolites, eclogites, etc. may have very low si, but quartz mica schists, gneisses, quartzites, etc. have si ranging up to values far in excess of igneous rocks.

k chart

With the exception of lamproite and missourite, the k of igneous rocks decreases with increasing X (Fig. 5), and the potash series have higher k values than the soda series.

mg chart

The mg of igneous rocks increases with increasing X, and is generally higher in the alkali lime series than in the alkali series for any selected value of X (Fig. 5).

Triangle Views of the Tetrahedron

The ratios of any of the bases to one another can be shown graphically by viewing the tetrahedron from the following six positions (Figs. 10, 11, and 12):

c/fm chart: tetrahedron viewed parallel to the al-alk edge gives the c/fm ratio.

alk/al chart: tetrahedron viewed parallel to the c-fm edge gives the alk/al ratio

alk/c chart: tetrahedron viewed parallel to the al-fm edge gives the alk/c ratio

al/c chart: tetrahedron viewed parallel to the alk-fm edge gives the al/c ratio

al/fm chart: tetrahedron viewed parallel to the alk-c edge gives the al/fm ratio

fm/alk chart: tetrahedron viewed parallel to the c-al edge gives the fm/alk ratio

These views are isosceles triangles of altitude equal to the side of the square top view, and of base equal to the diagonal. To obtain the projection point of a rock analysis in one of the triangles follow the line of given ratio until it intersects the altitude line, the latter representing the sum of the other two components. The intersection is the desired point.

As an example, the triangle positions of Becke's granite are calculated from the X 31, Y 53 and Z 38 coordinates.

$$\text{al} = \frac{100 - 31 + 53 - 38}{2} = 42$$

$$\text{fm} = \frac{31 - 53 - 38 + 100}{2} = 20$$

$$\text{c} = \frac{31 + 53 + 38 - 100}{2} = 11$$

$$\text{alk} = \frac{100 - 31 - 53 + 38}{2} = 27.$$

The positions of the granite point in the triangles lie at the intersections of the following ratio and altitude lines:

Chart	Ratio	Altitude
c/fm	c:fm =35:65	100−X=69
alk/al	alk:al =39:61	X=31
alk/c	alk:c =71:29	100−Z=62
al/c	al:c =79:21	100−Y=47
al/fm	al:fm =68:32	Z=38
fm/alk	fm:alk=43:57	Y=53

The alternate triangles are turned upside down for illustrative convenience. The altitude is always measured from the base or long side of the triangle toward the peak with the two components.

The triangle views are readily constructed and demonstrate certain rock relationships that are not expressed in the XYZ diagram.

c/fm chart (Fig. 10)

Igneous Rocks.—The field of the igneous rocks is bounded by the al-alk/fm edge and lines connecting anorthite with augite and fm. The c-fm ratio of .35 plus or minus .10 is characteristic for the major portion of both series of igneous rocks. Exceptions are anorthosite, the high c-fm ratio of which is due to abundant plagioclase feldspar; peridotite, the low c-fm ratio of which is due to the abundance of ferromagnesian constituents such as olivine, orthorhombic pyroxene and magnetite; and alkali granite with a low c-fm ratio owing to the scarcity and low lime

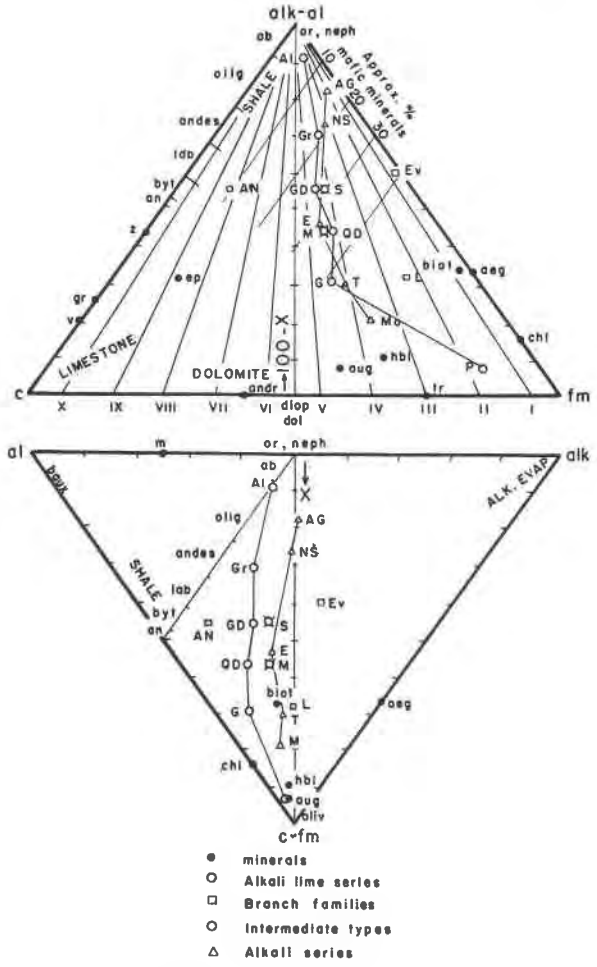

FIG. 10. Triangle views of the tetrahedron: c/fm and alk/al charts.

Mineral abbreviations: ab albite, aeg aegirite, an anorthite, andes andesine, andr andradite, aug augite, baux bauxite, biot biotite, byt bytownite, chl chlorite, diop diopside, dol dolomite, ep epidote, gr grossularite, hbl hornblende, lab labradorite, m muscovite, neph nepheline, olig oligoclase, oliv olivine, or orthoclase, tr tremolite, v vesuvianite, z zoisite.

Rock abbreviations: AG alkali granite, Al alaskite, AN anorthosite, E essexite, Ev evisite, G gabbro, GD granodiorite, Gr granite, L lamproite, M monzonite, Mo missourite, NS nepheline syenite, P peridotite, QD quartz diorite, S syenite, T theralite.

content of the plagioclase. The extremely alkaline nature of evisite is indicated by its low c-fm ratio. Lamproite has a low c-fm ratio.

From alkali feldspar rocks to diorite the approximate AbAn ratios of the plagioclase feldspars can be determined by dropping lines from fm through the rock analysis points to the plagioclase line. This is true also for anorthosite.

The percentage of mafic constituents can be estimated satisfactorily up to 40% by determining the altitude of the analysis point relative to the c/alk-al edge as a base.

This chart illustrates the planes along which Niggli cut the tetrahedron.

Sedimentary Rocks.—The sediments lie along the c/alk-al edge, limestone and gypsum at c, and the clays and shales nearer alk-al. The alkali evaporites also lie at alk-al. Dolomite is on the middle of the c-fm edge. Except for the iron ores, the distribution field of the sediments overlaps the igneous field very little.

Metamorphic Rocks and Processes.—Epidotization exhibits an increase of lime. Serpentinization involves a shift toward fm due to a loss of all but iron and magnesia. Chloritization, zoisitization and garnetization can also be demonstrated with this chart.

alk/al chart (Fig. 10)

Igneous Rocks.—The field of the igneous rocks is in the central portion of the triangle between the feldspar line and a line joining aegirite with orthoclase. The alkali lime series has an alk-al ratio under .40 (with the exception of alaskite), and the alkali series has an alk-al ratio over .40 (with the exception of missourite). The relation of lamproite and evisite to the alkali series is expressed by an alk-al ratio above normal for the series. The relation of anorthosite to gabbro is shown by the fact that it has the same alk-al ratio, but the higher plagioclase content draws the point toward basic plagioclase. The intermediate positions of monzonite and syenite are indicated by their analysis points.

Bowen's reaction series finds expression in the nearly vertical line from olivine through augite, hornblende and biotite to orthoclase, and by the plagioclase line from anorthite to albite, the two lines converging in the middle of the alk-al edge.

Sedimentary Rocks.—Most sediments have low alk-al ratios and lie close to the al/c-fm edge, but they coincide in part with the igneous field. Alkali evaporites lie at the alk corner.

Metamorphic Rocks and Processes, and Weathering.—Sericitization and kaolinization are expressed by shifts towards the muscovite point and al respectively.

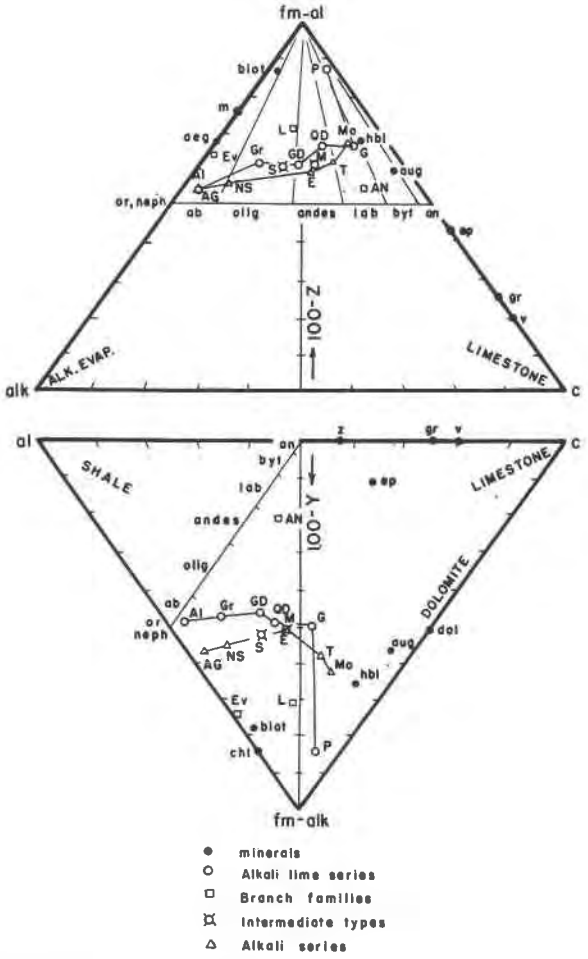

FIG. 11. Triangle views of the tetrahedron: alk/c and al/c charts.

Mineral abbreviations: ab albite, aeg aegirite, an anorthite, andes andesine, andr andradite, aug augite, baux bauxite, biot biotite, byt bytownite, cal calcite, dol dolomite, ep epidote, gr grossularite, hbl hornblende, lab labradorite, m muscovite, neph nepheline, olig oligoclase, or orthoclase, v vesuvianite, z zoisite.

Rock abbreviations: AG alkali granite, Al alaskite, AN anorthosite, E essexite, Ev evisite, G gabbro, GD granodiorite, Gr granite, L lamproite, M monzonite, Mo missourite, NS nepheline syenite, P peridotite, QD quartz diorite, S syenite, T theralite.

alk/c chart (Fig. 11)

Igneous Rocks.—The field of the igneous rocks lies between the feldspar line and the fm-al corner. Prevalence of alkali feldspar is marked by a high alk-c ratio. Increasing amounts of soda-lime feldspar cause a reduc-

tion of the alk-c ratio down to gabbro. At the gabbro point the igneous rock curve bends sharply toward fm as it approaches peridotite. Evisite lies between the soda amphiboles (aegirite and riebeckite) and alkali feldspar. Anorthosite lies between normal gabbro and labradorite. Olivine (and phlogopite) cause lamproite to have higher fm-al than normal phonolites or trachytes.

The chart gives the best estimates of the AbAn ratios of the plagioclase feldspars in the igneous rocks. In the case of orthoclase- and plagioclase bearing rocks the ratio is (OrAb)An.

Sedimentary Rocks.—Most sedimentary rocks have a low alk-c ratio and lie close to the fm-al/c line. The clays, laterites and iron ores lie at fm-al, dolomite at the anorthite point, and pure limestone at c. Rock salt and other alkali evaporites lie at alk.

Metamorphic Rocks and Processes, and Weathering.—Epidotization appears as a process involving an increase of lime, because epidote has a higher c than either anorthite or pyribole. Since the alk-c ratio of epidote is zero, there is also a slight loss of alk.

al/c chart (Fig. 11)

Igneous Rocks.—Prevalence of alkali feldspar is marked by a high al-c ratio, while increasing amounts of soda-lime feldspar accompanied by a reduction of alkali feldspar lower the ratio until in gabbro there is more lime than alumina. With the exception of peridotite, the alkali series is separated from the alkali lime series by higher fm-alk values. Anorthosite lies between normal gabbro and basic plagioclase. Evisite and lamproite show their relation to the alkali series by their high fm-alk values. The alkali lime series makes a sharp bend at the gabbro point due to the rapid decrease in plagioclase as the peridotite point is approached.

The igneous rock field is roughly diamond shaped, between fm-alk, orthoclase, anorthite and augite.

Sedimentary Rocks.—The major sediments lie along the al-c edge and are very effectively separated from the igneous rock field. Alkali evaporites and iron ores overlap the igneous field in the vicinity of the fm-alk corner.

Metamorphic Rocks and Processes.—Uralitization involves a loss of lime and gain in Mg which is indicated by the shift from augite to hornblende. Serpentinization, epidotization, garnetization and chloritization are also readily shown on this chart.

ol/fm chart (Fig. 12)

Igneous Rocks.—The field of the igneous rocks is defined by a triangle connecting the feldspars, fm and augite. The alkali lime series is distinctly separated from the alkali series by its lower Z, and syenite and mon-

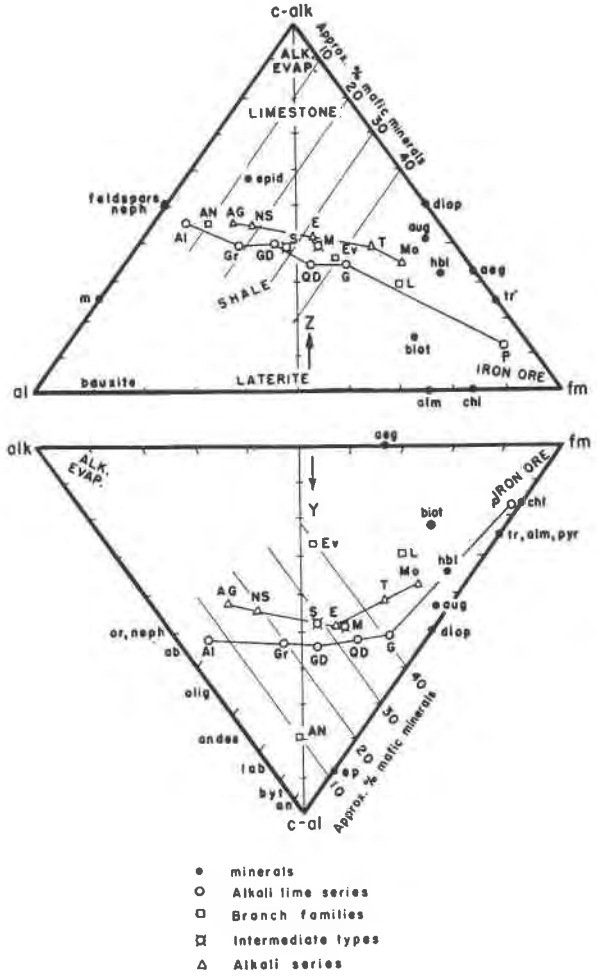

FIG. 12. Triangle views of the tetrahedron: al/fm and fm/alk charts.

Mineral abbreviations: ab albite, aeg aegirite, alm almandite, an anorthite, andes andesine, aug augite, biot biotite, byt bytownite, chl chlorite, diop diopside, ep epidote, hbl hornblende, lab labradorite, m muscovite, neph nepheline, olig oligoclase, or orthoclase, pyr pyrite, tr tremolite.

Rock abbreviations: AG alkali granite, Al alaskite, AN anorthosite, E essexite, Ev evisite, G gabbro, GD granodiorite, Gr granite, L lamproite, M monzonite, Mo missourite, NS nepheline syenite, P peridotite, QD quartz diorite, S syenite, T theralite.

zonite occupy intermediate positions.

The percentage of mafic constituents can be estimated up to 40% by determining the altitude of the analysis point relative to the al/c-alk edge as a base.

Sedimentary Rocks.—Except for the iron ores which lie near fm, the sediments range themselves between al and c-alk. There is only a slight overlap of the igneous field. Clays lie at al, pure limestones and alkali evaporites at c-alk, and the shales between.

Metamorphic Rocks and Processes, and Weathering.—The chart is adapted to illustrate the chemical changes involved in epidotization, sericitization, kaolinization, lateritization, chloritization and scapolitization.

fm/alk chart (Fig. 12)

Igneous Rocks.—The field of the igneous rocks lies between the fm/c-al edge and a line joining orthoclase and aegirite. The alkali series has Y under 50 and the alkali lime series has Y over 50 with the exception of peridotite. The relation of lamproite and evisite to the alkali series is shown by the high alk and low Y compared to the normal for the series. The anorthosite point lies between normal gabbro and basic plagioclase.

The percentage of mafic constituents can be estimated up to 40% by determining the altitude of the analysis point relative to the alk/c-al edge as a base.

Sedimentary Rocks.—The sediments occur bunched up at each of the corners. The most important corner is c-al where all gradations from limestone through calcareous shales to pure kaolin are located. Alkali evaporites lie at alk, and the iron ores at fm.

Metamorphic Rocks and Processes.—This chart may be used to illustrate chloritization, uralitization and serpentinization.

Conclusions

Any minerals or rocks containing one or more components of the quaternary chemical system al, fm, c and alk may be plotted as points in the Niggli-Becke tetrahedral system. The diagrams are suited for plotting chemical and modal analyses of all classes of rocks. The graphic nature and the broad adaptability of the projection for illustrating extremely varied petrochemical studies merits the recognition of all petrologists and students.

References Cited

Adams, F. D. (1914), Chemical relations of a petrographic province: *Jour. Geol.*, **22**, 689–693.

Becke, F. (1897), Gesteine der Columbrates: *Tschermak's miner. u. petrog. Mitt.*, **16**, 319.

——— (1912), Chemische Analysen von krystallinen Gesteinen aus der Zentralkette der Ostalpen: *Denkschriften d. math. naturwiss. Klasse d. k. Akad. d. Wissensch.*, Wien, **75**, 153.

——— (1925), Graphische Darstellung von Gesteinsanalysen: *Tschermak's miner. u. petrog. Mitt.*, **37**, 27–46.

BOEKE, H. E., AND EITEL, W. (**1923**), *Grundlagen der physikalisch-chemischen Petrographie*, 2nd ed., Berlin.

BROEGGER, W. C. (1895), Die Eruptionsfolge der triadischen Eruptivgestine bei Predazzo in Südtirol: *Videnskabs Selskabets Skrifter*, Kristiania, No. **7**, 55.

CLARKE, F. W. (1924), Data of Geochemistry: *U. S. Geol. Survey*, Bull. **770.**

DALY, R. A. (1910), Average chemical composition of igneous rocks: *Proc. Am. Acad. of Arts and Sci.*, vol. **45.**

DANA, E. S., AND FORD, W. E. (**1932**), *Textbook of Mineralogy*, New York.

GIBBS, J. W. (1876), Equilibrium of heterogeneous substances: *Trans. Conn. Acad.*, **3**, 176.

GROUT, F. F. (1918), A form of multiple rock diagrams: *Jour. Geol.*, **26**, 622–625.

——— (1922), Graphic study of igneous rock series: *Geol. Soc. Am., Bull.*, **33**, 617–638.

——— (1925), The Vermillion batholith of Minnesota: *Jour. Geol.*, **33**, 484–485.

GRUBENMANN, U., AND NIGGLI, P. (1924), *Die Gesteinsmetamorphose*, vol. **1**, Berlin.

HODGE, E. T. (1924), A proposed classification of igneous rocks. *Univ. of Oregon Publ.*, **2**, no. 7. Also in Johannsen (1932).

IDDINGS, J. P. (1892), Origin of igneous rocks: *Bull. Phil. Soc. Washington*, vol. **12.**

IDDINGS, J. P. (1903), Chemical composition of igneous rocks expressed by means of diagrams, with reference to rock classification on a quantitative chemico-mineralogical basis: *U. S. Geol. Survey*, Prof. Paper **18.**

JOHANNSEN, A. (1920), A quantitative mineralogical classification of igneous rocks, revised: *Jour. Geol.*, **28**, 38–60; 159–177; 210–232.

——— (1932, 1937, 1938), *A Descriptive Petrography of the Igneous Rocks*, Chicago, vols. **1, 2, 3,** and **4.**

LANG, H. O. (1892), Beiträge zur Systematik der Eruptivgesteine: *Tschermak's miner. u. petrog. Mitt.*, **13**, 160.

NIGGLI, P., AND BEGER, P. J. (1923), *Gesteins und Mineralprovinzen*, Berlin, vol. **1.**

OSANN, A. (1900), Versuch einer chemischen Classifikation der Eruptivgesteine: *Tschermak's miner. u. petrog. Mitt.*, **19**, 351–469.

PEACOCK, M. A. (1931), Classification of igneous rock series: *Jour. Geol.*, **39**, 54–67.

SCHUSTER, M. (1881), Ueber die optische Orientierung der Plagioklase: *Tschermak's miner. u. petrog. Mitt.*, vol. **3.**

TSCHERMAK, G., AND BECKE, F. (1920), *Lehrbuch der Mineralogie*, Wien.

VON WOLFF, F. (1922), Die Prinzipien einer quantitativen Klassifikation der Eruptivgesteine, insbesondere der jungen Ergussgesteine: *Geol. Rundschau*, **13**, 9–17. Also in Johannsen (1932).

WASHINGTON, H. S. (1917), Chemical analyses of igneous rocks: *U. S. Geol. Survey*, Prof. Paper **99.**

WINCHELL, A. N. (1933), *Elements of Optical Mineralogy*, Pt. **2**, p. 320.

TABLE 1. TABLE OF MINERALS GIVING SPECIFIC GRAVITIES, CHEMICAL FORMULAS, TETRAHEDRAL FACTORS, AND THE X, Y, Z AND si FACTORS WHICH REPRESENT THE MINERAL POSITIONS IN THE XYZ-si DIAGRAM

Mineral	Spec. Grav.	Chemical Formula	Tetr. Fact.	X	Y	Z	si
acmite	3.53	$Na_2O \cdot Fe_2O_3 \cdot 4SiO_2$	2.28	67	0	33	133
actinolite	3.1	$CaO \cdot 3(Mg, Fe)O \cdot 4SiO_2$	2.84	100	25	25	100
aegirite (acmite)			2.28	67	0	33	133
akermannite	3.18	$2CaO \cdot MgO \cdot 2SiO_2$	2.33	100	67	67	67
allanite (orthite: see epidote)			2.77	69	88	57	86
almandite	4.25	$3FeO \cdot Al_2O_3 \cdot 3SiO_2$	3.41	75	25	0	75
alunite	2.66	$K_2O \cdot 3Al_2O_3 \cdot 4SO_3 \cdot 6H_2O$	1.28	0	75	25	0
analcite	2.25	$Na_2O \cdot Al_2O_3 \cdot 4SiO_2 \cdot 2H_2O$	1.02	0	50	50	200
andalusite	3.18	$Al_2O_3 \cdot SiO_2$	1.97	0	100	0	100
andradite (melanite)	3.75	$3CaO \cdot Fe_2O_3 \cdot 3SiO_2$	3.68	100	60	60	60
anhydrite	2.95	$CaSO_4$	2.17	100	100	100	0
anthophyllite	3.03	$(Mg, Fe)O \cdot SiO_2$	2.81	100	0	0	100
antigorite (see serpentine)			2.78	100	0	0	67
apatite	3.2	$CaF_2 \cdot 3Ca_3(PO_4)_2$	3.1	100	100	100	0
apophyllite	2.35	$KF \cdot 4CaO \cdot 8SiO_2 \cdot 8H_2O$	1.31	89	89	89	178
arfvedsonite	3.45	$3Na_2O \cdot 8FeO \cdot Al_2O_3 \cdot 16SiO_2 \cdot 2H_2O$	2.22	67	8	25	133
augite (Average. Johannsen (1932))			2.92	93	43	41	98
bauxite	2.55	$Al_2O_3 \cdot 2H_2O$	1.85	0	100	0	0
beidellite	2.6	$Al_2O_3 \cdot 3SiO_2 \cdot 4H_2O$	0.73	0	100	0	300
beryl	2.7	$3BeO \cdot Al_2O_3 \cdot 6SiO_2$	2.01	75	25	0	150
biotite (Average. Johannsen (1932))			2.44	67	22	15	74
bronzite	3.25	$(Mg, Fe)O \cdot SiO_2$	2.88	100	0	0	100
calcite	2.71	$CaCO_3$	2.71	100	100	100	0
carnallite	1.60	$KCl \cdot MgCl_2 \cdot 6H_2O$	1.15	67	0	33	0
chabazite	2.12	$(Ca, Na_2)O \cdot Al_2O_3 \cdot 4SiO_2 \cdot 6H_2O$	0.82	25	75	50	200
chamosite	3.2	$15(Mg, Fe)O \cdot 5Al_2O_3 \cdot 11SiO_2 \cdot 16H_2O$	2.72	72	25	0	55
chondrodite	3.15	$Mg_2SiO_4 \cdot F_2Mg_3SiO_4$	4.15	100	0	0	40
chlorite	2.71	$4H_2O \cdot 5(Mg, Fe)O \cdot Al_2O_3 \cdot 3SiO_2$	2.94	84	16	0	50
chromite	4.5	$FeO \cdot Cr_2O_3$	4.01	50	50	0	0
collophanite	2.75	$Ca_3(PO_4)_2 \cdot H_2O$	2.75	100	100	100	0
cordierite	2.63	$2MgO \cdot 2Al_2O_3 \cdot 5SiO_2$	1.44	50	50	0	125
corundum	4.0	Al_2O_3	3.92	0	100	0	0
diallage (diopside)			3.04	100	50	50	100
diaspore	3.4	$Al_2O_3 \cdot H_2O$	2.83	0	100	0	0
diopside	3.29	$CaO \cdot MgO \cdot 2SiO_2$	3.04	100	50	50	100

TABLE 1—(*continued*)

Mineral	Spec. Grav.	Chemical Formula	Tetr. Fact.	X	Y	Z	si
dolomite	2.85	$CaCO_3 \cdot MgCO_3$	3.10	100	50	50	0
enstatite	3.15	$MgO \cdot SiO_2$	3.15	100	0	0	100
epidote	3.4	$H_2O \cdot 4CaO \cdot 3(Al, Fe)_2O_3 \cdot 6SiO_2$(Al:Fe=73:27)	2.77	69	88	57	86
epsomite	1.75	$MgSO_4 \cdot 7H_2O$	0.71	100	0	0	0
fluorite	3.18	CaF_2	4.07	100	100	100	0
gehlenite (melilite)	2.98	$3CaO \cdot Al_2O_3 \cdot 3SiO_2$	3.06	75	100	75	50
glauconite	2.5	$K_2O \cdot 2MgO \cdot 3(Fe,Al)_2O_3 \cdot 12SiO_2 \cdot 6H_2O$	1.34	56	33	11	133
glaucophane	3.07	$Na_2O \cdot Al_2O_3 \cdot 4SiO_2$	1.52	0	50	50	200
goethite	4.28	$Fe_2O_3 \cdot H_2O$	4.81	100	0	0	0
grossularite	3.53	$3CaO \cdot Al_2O_3 \cdot 3SiO_2$	3.13	75	100	75	75
gypsum	2.32	$CaSO_4 \cdot 2H_2O$	1.35	100	100	100	0
halite	2.16	NaCl	3.70	0	0	100	0
halloysite	2.1	$Al_2O_3 \cdot 2SiO_2 \cdot nH_2O$ (20%H_2O)	0.75	0	100	0	200
hedenbergite	3.55	$CaO \cdot FeO \cdot 2SiO_2$	2.86	100	50	50	100
hematite	5.2	Fe_2O_3	6.5	100	0	0	0
heulandite	2.2	$(Ca, Na_2)O \cdot Al_2O_3 \cdot 6SiO_2 \cdot 5H_2O$	0.73	25	75	50	300
hornblende (Average. Johannsen (1932))			2.92	89	34	32	91
hydrargillite (gibbsite)	2.35	$Al_2O_3 \cdot 3H_2O$	1.51	0	100	0	0
hypersthene	3.45	$(Fe, Mg)O \cdot SiO_2$	3.73	100	0	0	100
ilmenite	4.75	$FeO \cdot TiO_2$	3.13	100	0	0	0
kaolinite	2.61	$2H_2O \cdot Al_2O_3 \cdot 2SiO_2$	1.01	0	100	0	200
kyanite	3.61	$Al_2O_3 \cdot SiO_2$	2.23	0	100	0	100
leucite	2.48	$K_2O \cdot Al_2O_3 \cdot 4SiO_2$	1.14	0	50	50	200
limonite	3.8	$2Fe_2O_3 \cdot 3H_2O$	4.04	100	0	0	0
magnetite	5.17	$FeO \cdot Fe_2O_3$	7.22	100	0	0	0
margarite (Ca-mica)	3.04	$H_2O \cdot CaO_2 \cdot 2Al_2O_3 \cdot 2SiO_2$	2.28	33	100	33	67
marialite (scapolite)	2.62	$2NaCl \cdot 3(Na_2O \cdot Al_2O_3 \cdot 6SiO_2)$	0.99	0	43	57	257
meionite (scapolite)	2.77	$CaCO_3 \cdot 3(CaO \cdot Al_2O_3 \cdot 2SiO_2)$	2.21	57	100	57	86
melanterite	1.90	$FeSO_4 \cdot 7H_2O$	0.68	100	0	0	0
melilite (see gehlenite or akermannite)							
microcline and anorthoclase	2.55	$K_2O \cdot Al_2O_3 \cdot 6SiO_2$	0.92	0	50	50	300
montmorillonite	2.25	$MgO \cdot Al_2O_3 \cdot 5SiO_2 \cdot 6H_2O$	2.25	50	75	25	250
muscovite and sericite	2.88	$2H_2O \cdot K_2O \cdot 3Al_2O_3 \cdot 6SiO_2$	1.45	0	75	25	150
natrolite	2.23	$Na_2O \cdot Al_2O_3 \cdot 3SiO_2 \cdot 2H_2O$	1.17	0	50	50	150
nepheline	2.60	$Na_2O \cdot Al_2O_3 \cdot 2SiO_2$	1.82	0	50	50	100

TABLE 1—(*continued*)

Mineral	Spec. Grav.	Chemical Formula	Tetr. Fact.	X	Y	Z	si
olivine	3.32	$2(Mg, Fe)O \cdot SiO_2$	4.58	100	0	0	50
orthoclase and sanidine	2.55	$K_2O \cdot Al_2O_3 \cdot 6SiO_2$	0.92	0	50	50	300
paragonite (Na-mica)	2.84	$Na_2O \cdot 3Al_2O_3 \cdot 6SiO_2 \cdot 2H_2O$	1.49	0	75	25	150
pargasite (hornblende)	3.05	$CaO \cdot 2MgO \cdot Al_2O_3 \cdot 3SiO_2$	2.92	75	50	25	75
periclase	3.8	MgO	9.5	100	0	0	0
perovskite	4.0	$CaO \cdot TiO_2$	2.93	100	100	100	0
perthite (same as orthoclase or albite)							
phillipsite	2.2	$(K_2, Ca)O \cdot Al_2O_3 \cdot 4SiO_2 \cdot 4\frac{1}{2}H_2O$	0.90	25	75	50	200
phlogopite	2.81	$2H_2O \cdot K_2O \cdot 6MgO \cdot Al_2O_3 \cdot 6SiO_2$	2.70	75	13	13	75
plagioclase albite							
$Ab_{100}An_0$	2.62	$Na_2O \cdot Al_2O_3 \cdot 6SiO_2$	1.00*	0	50	50	300
$Ab_{95}An_5$	2.63		1.05	5	55	50	282
oligoclase $Ab_{90}An_{10}$	2.64		1.10	9	59	50	265
$Ab_{85}An_{15}$	2.65		1.15	13	63	50	248
$Ab_{80}An_{20}$	2.65		1.20	17	67	50	233
$Ab_{75}An_{25}$	2.66		1.25	20	70	50	222
andesine $Ab_{70}An_{30}$	2.67		1.30	23	73	50	208
$Ab_{65}An_{35}$	2.67		1.35	26	76	50	197
$Ab_{60}An_{40}$	2.68		1.40	29	79	50	186
$Ab_{55}An_{45}$	2.69		1.45	31	81	50	176
labradorite $Ab_{50}An_{50}$	2.69		1.50	33	83	50	166
$Ab_{45}An_{55}$	2.70		1.55	36	86	50	158
$Ab_{40}An_{60}$	2.71		1.60	38	88	50	149
$Ab_{35}An_{65}$	2.72		1.65	39	89	50	142
bytownite $Ab_{30}An_{70}$	2.72		1.70	41	91	50	136
$Ab_{25}An_{75}$	2.73		1.75	43	93	50	129
$Ab_{20}An_{80}$	2.73		1.80	44	94	50	122
$Ab_{15}An_{85}$	2.74		1.85	46	96	50	116
anorthite $Ab_{10}An_{90}$	2.75		1.90	47	97	50	111
Ab_5An_{95}	2.75		1.94	49	99	50	106
Ab_0An_{100}	2.76	$CaO \cdot Al_2O_3 \cdot 2SiO_2$	1.98	50	100	50	100
polyhalite	2.78	$2CaSO_4 \cdot MgSO_4 \cdot K_2SO_4 \cdot 2H_2O$	1.90	75	50	75	0
prehnite	2.88	$H_2O \cdot 2CaO \cdot Al_2O_3 \cdot 3SiO_2$	2.09	67	100	67	100
pyrite	5.03	FeS_2	4.20	100	0	0	0
pyrope	3.51	$3MgO \cdot Al_2O_3 \cdot 3SiO_2$	3.48	75	25	0	75
pyrophyllite	2.85	$H_2O \cdot Al_2O_3 \cdot 4SiO_2$	0.79	0	100	0	400

TABLE 1—(*continued*)

Mineral	Spec. Grav.	Chemical Formula	Tetr. Fact.	X	Y	Z	si
quartz and opal	2.66	SiO_2 (and $SiO_2 \cdot nH_2O$)	4.42** not plotted				
riebeckite	3.44	$Na_2O \cdot Fe_2O_3 \cdot 4SiO_2$	2.23	67	0	33	133
sanidine (see orthoclase)			0.92	0	50	50	300
scapolite (see marialite and meionite)							
scheelite	6.0	$CaWO_4$	2.08	100	100	100	0
scolecite	2.28	$CaO \cdot Al_2O_3 \cdot 3SiO_2 \cdot 3H_2O$	1.16	50	100	50	100
sericite (see muscovite)			1.45	0	75	25	150
serpentine	2.58	$3MgO \cdot 2SiO_2 \cdot 2H_2O$	2.78	100	0	0	67
siderite	3.86	$FeCO_3$	3.32	100	0	0	0
sillimanite	3.24	$Al_2O_3 \cdot SiO_2$	2.00	0	100	0	100
sodalite	2.22	$2NaCl \cdot 3(Na_2O \cdot Al_2O_3 \cdot 2SiO_2)$	1.61	0	43	57	86
soda niter	2.27	$NaNO_3$	1.33	0	0	100	0
spinel	3.8	$MgO \cdot Al_2O_3$	5.35	50	50	0	0
spodumene	3.17	$Li_2O \cdot Al_2O_3 \cdot 4SiO_2$	1.69	100	50	50	200
staurolite	3.71	$H_2O \cdot 2FeO \cdot 5Al_2O_3 \cdot 4SiO_2$	2.84	29	72	0	57
talc	2.75	$3MgO \cdot 4SiO_2 \cdot H_2O$	2.18	100	0	0	133
titanite	3.48	$CaO \cdot TiO_2 \cdot SiO_2$	1.78	100	100	100	100
topaz	3.5	$Al_2F_2O_2 \cdot SiO_2$	1.90	0	100	0	100
tremolite	3.05	$CaO \cdot 3MgO \cdot 4SiO_2$	2.94	100	25	25	100
vesuvianite	3.4	$2H_2O \cdot 12CaO \cdot 3Al_2O_3 \cdot 10SiO_2$	3.16	80	100	80	67
wolframite	7.3	$(Fe, Mn)WO_4$	2.40	100	0	0	0
wollastonite	2.85	$CaO \cdot SiO_2$	2.46	100	100	100	100
xanthophyllite	3.05	$H_2O \cdot CaO \cdot 4MgO \cdot 3SiO_2$—45% $H_2O \cdot CaO \cdot MgO \cdot 3Al_2O_3$—55%	3.64	67	53	20	27
zircon	4.5	$ZrO_2 \cdot SiO_2$	2.46** not plotted				
zoisite	3.31	$4CaO \cdot 3Al_2O_3 \cdot 6SiO_2 \cdot H_2O$	2.54	57	100	57	86

* Note: The tetrahedral factor increases by 0.01 for each per cent increase of An, except for anorthite.

** These are si factors equivalent to the tetrahedral factors but not plotted in the tetrahedron. Zircon also has a zr factor of 2.46.

TABLE 2. AVERAGE COMPOSITIONS OF THE IGNEOUS ROCKS PLOTTED IN THE XYZ-si DIAGRAM

Rock Family	X	Y	Z	si	k	mg
ALKALI LIME SERIES						
Alaskite	9	52	45	487	48	9
Granite	31	53	38	335	44	35
Granodiorite	45	54	39	248	28	48
Quartz diorite	56	52	34	188	30	51
Gabbro	69	51	34	107	19	60
Peridotite	93	16	13	70	0	84
BRANCH FAMILIES						
Anorthosite	45	79	46	124	12	52
Lamproite	68	29	29	140	80	80
Evisite (pantellerite)	40	26	36	290	3	8
INTERMEDIATE TYPES						
Syenite	45	48	39	204	43	43
Monzonite	56	49	39	154	44	52
ALKALI SERIES						
Alkali granite	18	43	45	398	40	9
Nepheline syenite	27	45	44	171	30	22
Essexite	54	49	41	131	27	40
Theralite	70	42	38	96	19	42
Missourite	79	38	33	89	74	72

TABLE 3. NIGGLI'S MAGMA FAMILIES IN THE XYZ-si DIAGRAM

Series	Magma Group	Magma Types or Rock Families	X	Y	Z	si
Alkali lime series	Granitic	aplite granitic	13	52	46	460
		engadinitic, e. granitic	18	50	44	420
		yosemititic, y. granitic	17	56	43	350
		normal granitic	41	50	39	270
		granodioritic	40	56	38	270
		opdalitic (quartz monzonitic)	50	50	36	215
	Dioritic	trondhjemitic	23	53	46	350
		plagioclase granitic, oligoclasitic	32	58	42	310
		quartz dioritic	50	50	38	220
		tonalitic	55	55	34	200
		peleeitic	56	56	34	180
		normal dioritic	57	51	36	155
		gabbro-dioritic	65	48	33	135

TABLE 3—(*continued*)

Series	Magma Group	Magma Types or Rock Families	X	Y	Z	si
Alkali lime series	Gabbroid & Anorthositic	normal gabbroid	73	42	27	108
		pyroxenite-hornblende gabbroid	72	55	36	100
		ossipitic, o. gabbroid	63	57	37	110
		anorthosite gabbroid	55	70	41	130
		andesine-labradorite-felsic and anorthositic	40	80	46	145
	Ultra femic	issitic, ostraitic	82	44	34	75
		pyroxenitic	91	36	31	95
		koswitic	97	35	33	65
		hornblenditic	80	35	25	80
		hornblendite-pyroxenite-peridotitic	88	24	16	80
		orthaugitic	95	9	6	95
		peridotitic	94	9	5	60
Soda series	Alk. granitic pulaskitic	alkali granitic (soda granitic)	19	42	43	400
		nordmarkite-pulaskitic	20	46	44	250
		soda-quartz-syenitic, soda syenitic	39	42	39	200
		soda-lamprosyenitic	64	34	26	145
		evisitic	40	26	36	290
	Foyaitic	larvikitic and monzonite foyaitic	30	51	43	180
		normal foyaitic	17	47	46	190
		urtitic	16	45	49	116
		monmouthitic	28	54	50	100
		nosykombitic	42	47	39	150
		ijolitic	50	50	50	100
		melteigitic (theralitic-ijolitic)	64	51	49	90
		lujavritic, agpaitic	33	34	43	160
	Essexitic	toensbergitic or essexite-dioritic	37	55	42	180
		essexitic (normal essexitic)	50	50	40	130
	Theralitic or Alk. gabbroid	theralitic	65	42	39	100
		theralite gabbroid	69	43	34	90
		essexite gabbroid	67	47	34	105
		jacupirangitic	91	42	37	70
Potash series	Quartz-syenitic or Granite-syenitic	rapakiwitic	27	49	41	380
		granosyenitic	27	50	43	260
		adamellitic	36	50	40	330
		tasnagranitic	36	43	37	290
		syenite granitic	41	42	41	250

TABLE 3—(*continued*)

Series	Magma Group	Magma Types or Rock Families	X	Y	Z	si
Potash series	Syenitic	juvitic or leuco-syenitic	25	51	46	178
		vesuvitic	40	53	47	160
		monzonite syenitic	37	51	40	190
		normal syenitic	45	45	40	185
		lamprosyenitic-lampromonzonite syenitic	58	37	29	160
		lamprosommaitic	62	43	31	140
		lamproitic (Wyoming type)	55	32	41	165
		lamproitic (Murcia type)	68	29	29	140
		borolanitic	52	57	51	130
	Monzonitic	normal monzonitic	51	51	40	140
		sommaitic	61	51	42	115
		sommaitic dioritic	67	48	35	130
		yogoitic, y. monzonitic	58	44	40	145
	Shonkinitic	normal shonkinitic	70	41	37	105
		missouritic	74	48	44	95
		pyroxenolitic	83	56	47	80

TABLE 4. SEDIMENTARY ROCKS PLOTTED IN THE XYZ-si DIAGRAM

Name of rock or sediment	X	Y	Z	si
Composite analysis of 345 limestones (Clarke 1924; p. 564)	99	79	78	9
Composite analysis of 498 limestones used for building purposes (Clarke 1924; p. 564)	91	73	78	23
Composite of 51 Paleozoic shales (Clarke 1924; p. 552)	45	48	20	257
Composite of 27 Mesozoic and Cenozoic shales (Clarke 1924; p. 552)	56	55	37	210
Cretaceous shale (highly calcareous), Mt. Diablo, Calif. (Clarke 1924; p. 552)	89	78	67	56
Composite analysis of 253 sandstones (Clarke 1924; p. 547)	68	68	56	618
Composite analysis of 371 sandstones used for building purposes (Clarke 1924; p. 547)	41	54	31	990
Granite laterite (Clarke 1924; p. 498)	17	83	0	248
Diorite laterite (Clarke 1924; p. 498)	34	66	0	4
Laterite F. India (Clarke 1924; p. 498)	73	27	0	tr
Marine red clay (23 analyses) (Clarke 1924; p. 516)	58	47	5	276
Marine red mud (Clarke 1924; p. 517)	80	79	72	75

TABLE 5. METAMORPHIC ROCKS PLOTTED IN THE XYZ-si DIAGRAM

Name of rock	X	Y	Z	si
Serpentine A (Clarke 1924; p. 617)	98	3	1	66
Lime silicate hornfels (Grubenmann and Niggli 1924; p. 260)	81	48	42	120
Epidosite (Clarke 1924; p. 610)	74	74	51	92
Amphibolite (Grubenmann and Niggli 1924; p. 496)	74	40	32	90
Greenstone with hornblende, albite and chlorite (Grubenmann and Niggli 1924; p. 488)	73	40	24	104
Plagioclase diopside hypersthene hornfels (Grubenmann and Niggli 1924; p. 486)	71	42	31	118
Eclogite, Tirol (Grubenmann and Niggli 1924; p. 405)	71	48	33	92
Glaucophane schist (Grubenmann and Niggli 1924; p. 497)	63	23	26	139
Lime silicate hornfels (Grubenmann and Niggli 1924; p. 260)	61	30	18	151
Plagioclase hypersthene hornfels (Grubenmann and Niggli 1924; p. 486)	59	46	26	162
Lime silicate hornfels (Grubenmann and Niggli 1924; p. 260)	51	23	21	157
Quartzite A (Clarke 1924; p. 619)	50	38	18	410
Quartz, two mica garnet schist; average of 6 analyses (Grubenmann and Niggli 1924; p. 485)	46	47	26	244
Andalusite schist A (Clarke 1924; p. 625)	45	49	17	275
Staurolite biotite schist (Grubenmann and Niggli 1924; p. 495)	38	61	9	72
Quartz-muscovite-chlorite-phyllite; average of 8 analyses (Grubenmann and Niggli 1924; p. 485)	37	50	19	231
Feldspathic mica schist (Clarke 1924; p. 626)	31	50	35	342
Quartzite C (Clarke 1924; p. 619)	30	53	20	1910
Biotite orthoclase gneiss (Grubenmann and Niggli 1924; p. 391)	27	50	41	376
Andalusite-cordierite-hornfels (Grubenmann and Niggli 1924; p. 486)	22	58	29	291